CLIMATE CHANGE-INDUCED RANGE SHIFTS IN CHINESE ASH (*FRAXINUS CHINENSIS*) ALONG THREE GEOGRAPHICAL DIMENSIONS IN CHINA AT THE LATE 21ST CENTURY

LI, G. Q.[1*] – AN, K. L.[2] – LI, Y. R.[2]

[1]*State Key Laboratory of Soil Erosion and Dryland Farming on the Loess Plateau, Institute of Soil and Water Conservation, Northwest A&F University, Yangling, Xianyang 712100, China*

[2]*College of Forestry, Northwest A&F University, Yangling, Xianyang 712100, China*

**Corresponding author*
e-mail: liguoqing@nwsuaf.edu.cn; phone: +86-29-8701-2411; fax: +86-29-8701-2210

(Received 12th May 2022; accepted 26th Jul 2022)

Abstract. In the present study, we establish a set of indicator systems to characterize the shifts in total range and core range of Chinese ash (*Fraxinus chinensis*) at three geographical dimensions under climate change scenarios in China by the year of 2070. The results show that current core range and total range areas were 1.3×10^6 km^2 and 3.3×10^6 km^2, accounting for 13.5% and 34.4% of the land area in China. The size of core range and total range areas will increase in varying degrees, depending on the CO2 emission concentration path. The average of future core range and total range areas were 1.95×10^6 km^2 and 3.7×10^6 km^2 across climate change scenarios, accounting for 20.3% and 38.5% of the land area in China. But, there was a difference in the centroid shift velocity and direction between the core and total ranges at the horizontal gradient. The average shift speed of total range is 11.39 km/decade toward northwest and that for core range is 9.32 km/decade toward northeast across climate scenarios. The average shift speed of the core range -9.05 m/decade downward and that for total range is 17.15 m/decade upward across climate change scenarios. This study indicates that the response of total range and core distribution range to climate change is not synchronous. Considering poleward or northward shift will underestimate about 2.2-20.1% for total range and 21.2-56.3% for core range. Thus, the study have important guiding significance for determining the potential shift route and adjust the shift speed for planting the tree species in response to future climate change. The indicator systems used here have a wide range of practicability and can applied to any species, region, or time.
Keywords: *Fraxinus chinensis, shift velocity, bioclimatic envelope model, centroid method, forest management, suitable habitat*

Introduction

Global climate is changing with human interference; temperature and rainfall patterns have changed dramatically, which will inevitably lead to changes in the structure and function of natural ecosystems at different organizational levels (Geest et al., 2018; Zhang et al., 2019). At the species level, the shift in species range, rather than evolution and extinction, are currently considered the most likely strategy for adapting to climate change (Aitken et al., 2008; Kosanic et al., 2019). Many biological taxa have shifted their ranges along latitudinal and altitudinal gradients in the past few decades (Chen et al., 2011) and the direction of shifts in ranges is mainly related to temperature gradient (Lenoir et al., 2008; Lenoir and Svenning, 2015). However, this is currently not fully demonstrated by many studies. Species can shifted and migrated in multiple directions because the limitation of species range is not only temperature, but also other environmental and biological variables (Aitken et al., 2008; Lafleur et al., 2010; Huang et al., 2018). In particular, species that are sensitive to both temperature and precipitation may move in other directions (Li et al., 2021; Harsch and

http://www.aloki.hu ● ISSN 1589 1623 (Print) ● ISSN 1785 0037 (Online)
DOI: http://dx.doi.org/10.15666/aeer/2005_44994513

HilleRisLambers, 2016). Besides, due to the location relationship between land, ocean, mountain and plateau, the distribution patterns of temperature and precipitation gradient will affect the velocity and direction of range shift for particular species (Burrows et al., 2014; Huang et al., 2018).

For the protection, management, and introduction of specific species in the context of climate change, it is necessary to quantitatively characterize the potential distribution range (Li et al., 2020), as well as the likely range shift velocity and direction of the species (Iverson et al., 2008), which are crucial for our understanding of whether the species can keep up with climate change in the natural state, and knowing where there is still afforestation potential and where the species will face threats under future climate change conditions (Booth, 2016). The basic method of characterizing the potential range of species is mainly based on the climate envelope modeling (Booth et al., 2014; Gobeyn et al., 2019). A climate envelope model quantitatively characterizes the realized climatic niche of the species based on the relationship between the species occurrence data and the climate variables, and then applies the realized climatic niche onto current and future scenarios to project the current and future ranges (Peterson et al., 2011).

Characterizing velocity and direction of range shift is usually performed using the centroid method (Huang et al., 2016, 2018), which mainly calculates the latitude, longitude, and altitude centroids of the current and future potential distribution ranges, and estimates the direction and velocity of range shifts through certain calculations. However, a global meta-analysis have shown that few studies used a multidimensional approach focusing on at least two geographical dimensions (e.g. latitude and elevation) simultaneously to assess range shifts at the leading edge, the trailing edge or the optimum position (Lenoir and Svenning, 2015). What is more, previous studies have focused more on the total range and less on the core range of species (Huang et al., 2017, 2018; Robinson et al., 2015). Whether the dynamics of the core range is consistent with that of the total range remains to be studied for many target species, as the dynamics of core range play an important role in the construction of nature reserves or seedling breeding centers for protection and utilization purpose.

Chinese ash (*Fraxinus chinensis*) is a deciduous tree, which has major commercial use for breeding Ericerus pela to produce white wax, as well as used for woody products and traditional Chinese medicine (DFRPSAASE, 1994). Due to its strong sprout capacity and salt and drought tolerance (Ren et al., 2022), the species has a significantly ecological use for mountain soil conservation and urban greening projects (Zhang et al., 2022). With the improvement of urbanization level (Yang and Wang, 2019) and the strengthening of ecological restoration projects in China (Bryan et al., 2018), Chinese ash has been widely introduced to many regions of China. Numbers of breeding bases have also been established across the country. All these facts indicate the natural dispersal is not a limit factor in determining the species distribution. Previous studies investigated the reproductive technology (Xu and Ye, 2014; Zhang et al., 2007), pest control (Diao and Ding, 2004; Ma, 2022), and physiological response (Zhang et al., 2022), which have contributed greatly to the conservation and rational use of Chinese ash. In terms of the response of this species to climate change, Wang et al. (2012) suggested that Chinese ash had a phenological response with an average advance of 1.1 days/decade during 1952 to 2007 in ten years. However, the way in which future climate change is likely to affect the range shifts of this species along three geographical dimensions is still unknown, which is essential for development of climate change adaptation strategies for the species.

http://www.aloki.hu ● ISSN 1589 1623 (Print) ● ISSN 1785 0037 (Online)
DOI: http://dx.doi.org/10.15666/aeer/2005_44994513

Here we established a set of indicator systems to characterize the shifts in total range and core range at three geographical dimensions for Chinese ash (*Fraxinus chinensis*) under future climate change based on the bioclimatic envelope model and centroid method. The aims of this study were to 1) estimated the current and future total and core ranges of Chinese ash in China, 2) characterized the velocity and direction of total and core range shifts under future climate. This study theoretically makes sense for describing the three-dimensional range shift dynamics to elucidate the response of species to climate change. In practice, it is of great significance for the adaptive management of Chinese ash to cope with climate change.

Materials and methods

Species and climate databases

Occurrence data

The specimen data for Chinese ash was obtained from the Chinese Virtual Herbarium (http://www.cvh.ac.cn, 2382 specimens) and Global Biodiversity Information Facility (http://www.gbif.org, 1426 specimens) databases. The duplicate specimens and specimens without locational information or coordinates were removed. Then, the remaining specimens were rasterized onto a raster layer with 10-arcmin resolution. Currently, there is a general assumption that specimen data can represent the climatic requirements of the species in the study of species distribution models (Soberon and Nakamura, 2009; Booth, 2018). Here, a grid cell was considered a suitable habitat when one or more specimens were located in it. However, it is an open question whether a grid cell could be defined as suitable habitat if only one individual lives there. This is beyond the scope of this study. Finally, the binary occurrence map with 10-arcmin resolution was converted into points, and we obtained 293 records with latitudinal and longitudinal values (DOI: 10.6084/m9.figshare.19736284.v1).

Climatic variables

We integrated a set of climatic factors based on BIOCLIM (Hijmans et al., 2005; Booth, 2018), Holdridge life zone model (Holdridge, 1947) and Kira's index system (Kira, 1945). An excess of climatic factors can cause overfitting for simulating process, so we only selected 8 of the 19 BIOCLIM variables based on our previous research. A total of 13 climatic factors were used to define the climatic niches of in China, which were widely used in research on the relationship between species/vegetation and climate, at a regional or global scale (e.g. Li et al., 2018; Huang et al., 2018). The 13 climatic variables are introduced in Table 1.

Current and future climate layers

The basic climatic layers of current and future climate scenarios were obtained from the WorldClim database (http://www.worldclim.org/). In the database, the current climatic layers were generated from thin plate smoothing splines using latitude, longitude, altitude, monthly temperature, and precipitation data from the averages of 51-year (1950–2000) climate station records (Hijmans et al., 2005).

The future climatic layers were generated from many general circulation models (GCMs) with four representative concentration pathways (RCP2.6, RCP4.5, RCP6.0,

http://www.aloki.hu ● ISSN 1589 1623 (Print) ● ISSN 1785 0037 (Online)
DOI: http://dx.doi.org/10.15666/aeer/2005_44994513

and RCP8.5). Here, the climatic layers of future scenarios were averaged by combining seven GCMs to deal with the uncertainty of GCMs under four representative concentration pathways (Huang et al., 2018). The seven GCMs were from seven modeling centers of six countries: BCC-CSM1-1, CCSM4, GISS-E2-R, HadGEM2-AO, IPSL-CM5A-LR, MIROC-ESM-CHEM, and NorESM1-M.

Table 1. *Description of 13 climatic variables*

Nr.	Variable	Abbreviation	Unit
1	Annual mean temperature	AMT	°C
2	Maximum temperature of the warmest month	MTWM	°C
3	Minimum temperature of the coldest month	MTCM	°C
4	Annual range of temperature	ART	°C
5	Annual precipitation	AP	mm
6	Precipitation of the wettest month	PWM	mm
7	Precipitation of the driest month	PDM	mm
8	Precipitation of seasonality	PSD	mm
9	Annual biotemperature	ABT	°C
10	Warmth index	WI	°C
11	Coldness index	CI	°C
12	Potential evapotranspiration rate	PER	/
13	Humidity index	HI	mm/°C

The time-period from 2061 to 2080 was selected as the target future, in which the annual temperature in China will increase from 6.4 °C to 8.2–10.6 °C and the annual precipitation will increase from 576 mm to 603–623 mm based on ensemble average results of the seven GCMs in contrast to that of 1950-2000. All climatic layers used be obtained from DOI: 10.6084/m9.figshare.19736284.v1.

Simulation and range shift calculation processes

Simulation process

We used a Maxent model as a bioclimatic envelope model to simulate the current and future range of Chinese ash under current and future scenarios in China (Phillips et al., 2006; Elith et al., 2010). MaxEnt is a machine learning algorithm written in Java, and it can be used on all modern computing platforms. The software is freely available on the Internet (https://biodiversityinformatics.amnh.org/open_source/maxent/). The Maxent performance was evaluated using 10-fold cross-validation of all records and characterized by the area under the receiver operating characteristic curve (AUC) and predicted accuracy (Fielding and Bell, 1997). A jackknife test (systematically leaving out each variable) and the regularized gain change [log of the number of grid cells minus the log loss (average of the negative log probabilities of the sample locations)] were then used to evaluate which climatic factors were the most important in determining the climatic suitability of the species.

In this study, the Maxent model expresses the climatic suitability of a grid cell as a function of its 13 climatic variables in China together, with 293 sample records where the species was observed, where the climatic suitability takes the form (*Eq. 1*):

http://www.aloki.hu ● ISSN 1589 1623 (Print) ● ISSN 1785 0037 (Online)
DOI: http://dx.doi.org/10.15666/aeer/2005_44994513

$$P(x) = \exp(c_1 \times f_1(x) + c_2 \times f_2(x) + c_3 \times f_3(x) + ...) / Z \quad \text{(Eq.1)}$$

where c_1, c_2, c_3,… are constants; f_1, f_2, f_3,… are the features (or variables), and Z is a scaling constant that ensures that P sums to 1 over all grid cells. Then, the simulated Maxent models were projected on the current and future climate scenarios to obtain five suitability maps for Chinese ash, with one map of the current condition and four maps of future conditions.

We converted the five climatic suitability maps into two types of maps: total range maps and core range maps. The total range maps were converted from these climatic suitability maps with an optimal threshold of maximum sensitivity and specificity [max(tp/(tp + fn) + tn/(tn + fp)), tp is true positive value, fn is false negative value, fp is false positive value and tn is true negative value] (Fielding and Bell, 1997). The core range maps were also generated from climatic suitability maps with two times the optimal threshold. Finally, we obtained 10 range maps with five total range maps and five core range maps, each with one current map and four maps for four RCPs.

Range shift calculation process

The change in size of area under current and future scenarios was characterized by three indices: the expansion area, loss area, and stability area, which were calculated by the sum of the area of each occurring grid cell. The centroids of species range at three geographical dimensions were computed based on the following formulae (*Eqs. 2–4*):

$$Lon_c = \sum_{i=1}^{n} (Lon_i / n) \quad \text{(Eq.2)}$$

$$Lat_c = \sum_{i=1}^{n} (Lat_i / n) \quad \text{(Eq.3)}$$

$$Alt_c = median(Alt_i) \quad \text{(Eq.4)}$$

where Lon_c, Lat_c, and Alt_c represent the longitude, latitude and altitude centroids on the range map (using Geographic Coordinate System: GCS_WGS_1984; Angular Unit: degree), respectively, and n represents the number of occurring grid cells. The reason we used arithmetic means for longitude and latitude, but median for altitude was that occupancy grids value of longitude and latitude generally shows normal distribution pattern, while that of altitude value generally shows skewed distribution pattern.

The shift velocities of range centroids along the longitudinal, latitudinal, and vertical directions were calculated using the following formulae (*Eqs. 5–7*):

$$SV_{lon} = (Lon_f - Lon_c) / n \quad \text{(Eq.5)}$$

$$SV_{lat} = (Lat_f - Lat_c) / n \quad \text{(Eq.6)}$$

$$SV_{alt} = (Alt_f - Alt_c) / n \quad \text{(Eq.7)}$$

where SV_{lon}, SV_{lat}, and SV_{alt}, represent shift velocities of range centroids along the longitudinal, latitudinal, and vertical directions. Lon_f, Lat_f, Lon_c, Lat_c, represent the

http://www.aloki.hu ● ISSN 1589 1623 (Print) ● ISSN 1785 0037 (Online)
DOI: http://dx.doi.org/10.15666/aeer/2005_44994513

longitude and latitude of centroids under future and current climate scenarios (using Projected Coordinate System: Clarke_1866_Albers; Linear Unit: meter), respectively. Alt_f and Alt_c represent the altitudes of centroids under future and current climate scenarios, respectively. The divisor n represent the time period between current and target future scenarios [the median value of 1950-2000 (current period, 1975) and 2060-2080 (future period, 2070) were used to determine n value (9.5 decades) in this study]. The total shift velocities (SV) of ranges on earth surface were calculated using the following formula (*Eq. 8*):

$$SV = \sqrt{SV_{lon}^2 + SV_{lat}^2} \quad \text{(Eq.8)}$$

We also calculated the altitude changes along the longitudinal and latitudinal gradients (the range of the species was divided into bands with one-degree width along the two gradients, and the median value of altitude in each band represented the centroid of that band. All statistical analyses were performed on R software.

Results

Maxent performance and total and core distributions of Chinese ash

The results of the ten cross-validations showed that the Maxent prediction accuracy is high. The test AUC reached 0.83, and the prediction accuracy rate was 71%. We found that MTCM, AP, and CI were the most important climatic factors determining the distribution of Chinese ash. The three factors could explain 84% of the variance, and could be divided into thermal group (MTCM and CI, 59.5%) and humidity group (AP, 24.5%). It appeared that thermal condition was more important than humidity condition in controlling the distribution ranges of the species.

Both climatic suitability map and total range map (optimal threshold is 0.26) are shown in *Fig.1AB.* They show that the total range of Chinese ash spreads throughout almost all provinces in the southeast of China. The total range area can occupy 34.4% (3.3×10^6 km^2) of the land area in China. The core range map is generated from suitability maps with threshold of 0.52 (two times the optimal threshold, *Fig.1C*). It indicates that the core areas (with high suitability) are mainly concentrated in center part of China, occupying 13.5% (1.3×10^6 km^2) of the country's land area. The results of the ten cross-validations showed that the Maxent prediction accuracy is high. The test AUC reached 0.83 (*Fig. 1D*).

Range expansion and loss under future climate change scenarios

The increase or decrease of the future total range area and core range areas show that the overall range of Chinese ash is relatively stable in response to future climate change (*Fig.2*). The results show that the average of future core range and total range areas were 1.95×10^6 km^2 and 3.7×10^6 km^2 across climate change scenarios, accounting for 20.3% and 38.5% of the land area in China. The stable area occupies 3.0–3.2 $\times 10^6$ km^2 for the total range and 1.0–1.1 $\times 10^6$ km^2 for the core range of the species; the loss area occupies 0.1–0.26 $\times 10^6$ km^2 for total range and 0.17–0.21 $\times 10^6$ km^2 for the core range; the expansion area occupies 0.4–0.8 $\times 10^6$ km^2 for the total range and 0.7–1.1 $\times 10^6$ km^2 for the core range. Generally, the dynamics of suitability range were more sensitive at high concentration path (e.g. RCP8.5) than that of low concentrations path (e.g.

http://www.aloki.hu ● ISSN 1589 1623 (Print) ● ISSN 1785 0037 (Online)
DOI: http://dx.doi.org/10.15666/aeer/2005_44994513

RCP2.6). The location of expansion area in the total range was mainly distributed in the northern boundary and that of loss area was mainly distributed in the south boundary. The size of expansion area is larger than that of loss area in both core and total ranges of Chinese ash.

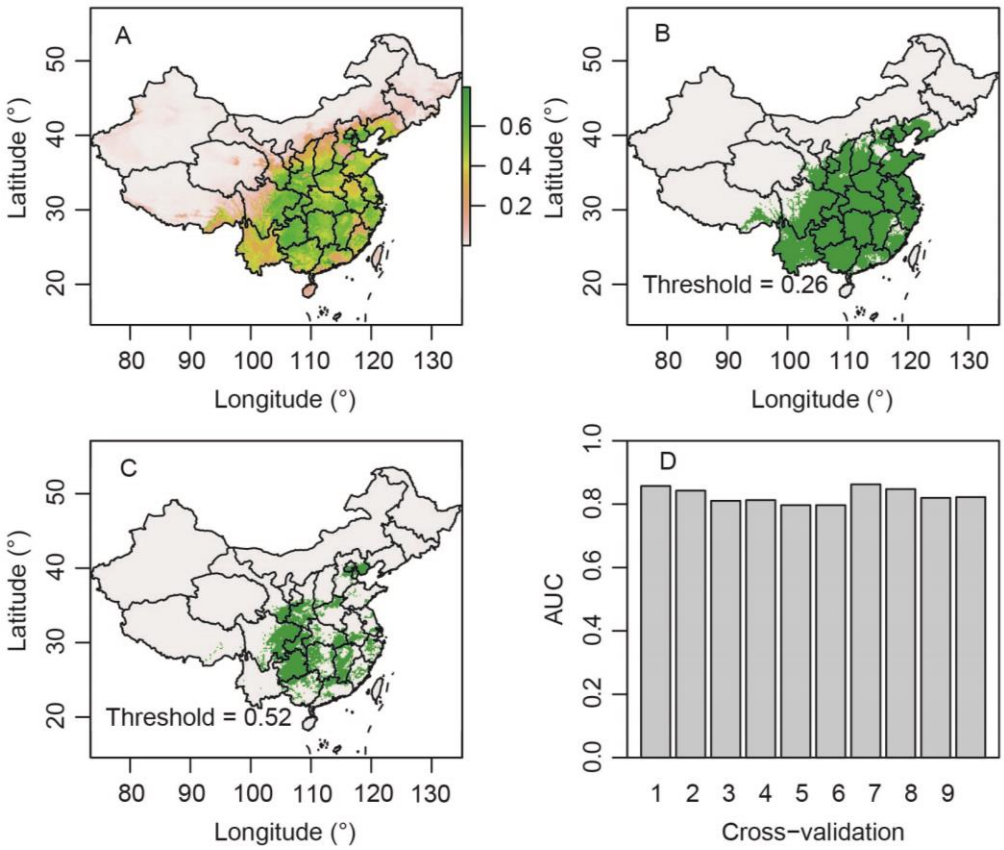

Figure 1. *Current climatic suitability maps based on all occurrence data and Maxent model. (A) Probability map; (B) Total range map (threshold = 0.26). (C) Core range map (threshold = 0.52). (D) Area under the receiver operating characteristic curve (AUC) of 10 cross-validations*

Centroid shifts along three geographical dimensions

The shift pattern of the total range and core range of Chinese ash in horizontal and vertical directions is shown in *Fig.3*. The results show that the centroid of total range is located in Changyang Tujia Autonomous County (*Fig.3A*), the future centroids will shift to the northwest, the shift velocity is 7.86–14.92 km/decade (1.65–8.76 km/decade along the longitudinal gradient; 7.49–12.08 km/decade along the latitudinal gradient); the centroid of the core range is located in Shimen County (*Fig.3C*), the future centroid will shift to the northeast, the velocity is about 6.30–12.33 km/decade (5.36–8.67 km/decade along longitudinal gradient; 3.30–9.72 km/decade along latitudinal gradient). The altitude will shift to a higher altitude in the total range, from 507.5 m in the current climate, to 585–755 m in the future climate (*Fig.3B*), with a centroid shift velocity of 8.2–26.1 m/decade. The altitude will shift to a lower altitude in the core range, from 505 m in current climate to 405–433 m in the future climate (*Fig.3D*), with a centroid shift velocity from -10.5 to -7.6 m/decade.

http://www.aloki.hu ● ISSN 1589 1623 (Print) ● ISSN 1785 0037 (Online)
DOI: http://dx.doi.org/10.15666/aeer/2005_44994513

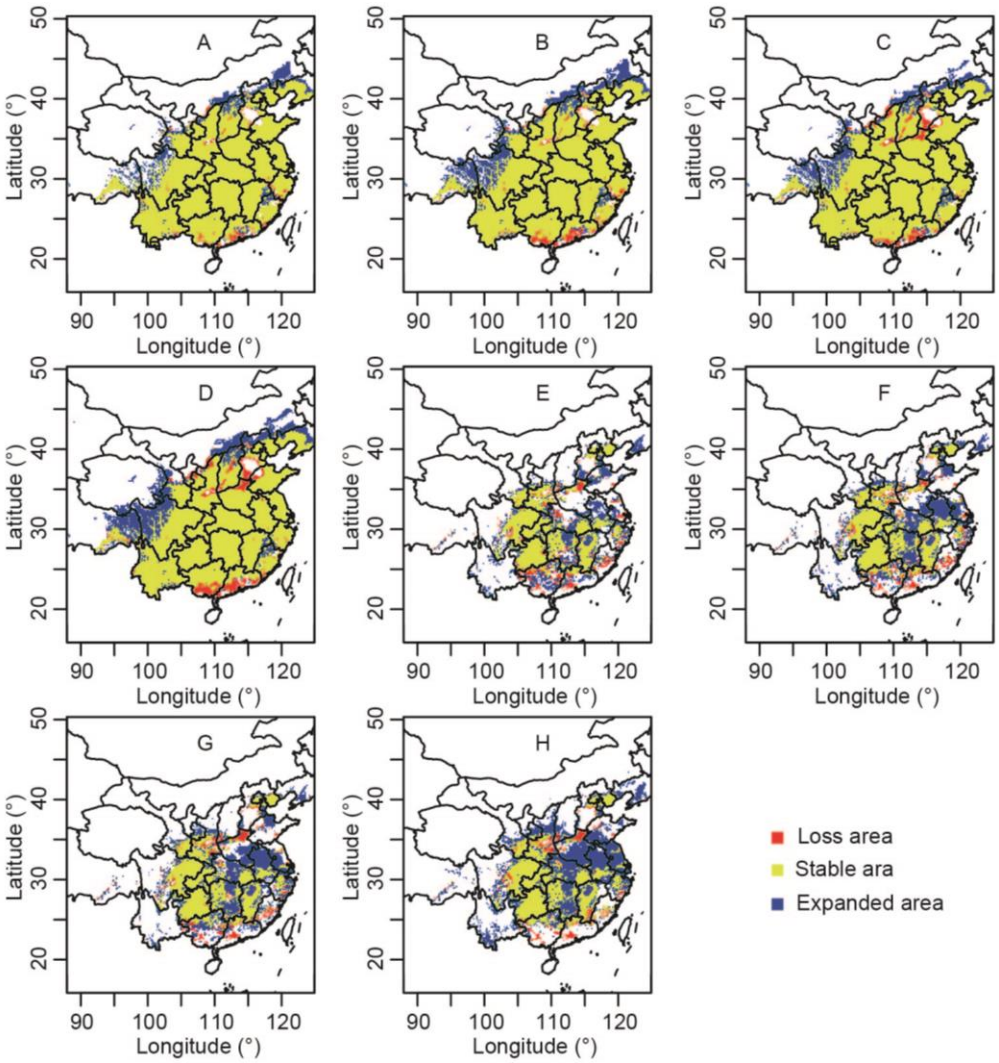

Figure 2. *Expansion of area, loss of area, and stability of area by overlap of current and future total range maps. Total range shift under RCP2.6 (A), RCP4.5(B), RCP6.0 (C) and RCP8.5(D); Core range shift under RCP2.6 (E), RCP4.5(F), RCP6.0 (G) and RCP8.5(H)*

We analyzed the altitude centroids along the longitudinal and latitudinal gradients in the total range and core range maps (*Fig.4*). It shows that there is no obvious rising trend along the longitudinal gradient, regardless of the core range or the total range (*Fig.4A, C*). In the latitudinal gradient, there was a significant trend in raising altitude in the total range maps, especially in the area where the latitude was higher than 30° (*Fig.4B*). In contrast, the shift of altitude in the core range has an upward or downward trend in the latitudinal gradient, but it is less violent than that for the total range (*Fig.4C*). Between 30–35°, there is a phenomenon of altitude decrease in the core range (*Fig.4D*).

Discussion

Climate change induced range shifts in three geographical dimensions

We studied the effects of climate change on the distribution of an afforestation tree species, Chinese ash, and established a procedure that describes the speed and direction

http://www.aloki.hu ● ISSN 1589 1623 (Print) ● ISSN 1785 0037 (Online)
DOI: http://dx.doi.org/10.15666/aeer/2005_44994513

of range shift in both total and core ranges for the target species in three geographical dimensions. Our study found that the size of total range area of Chinese ash will increase, mainly due to the increase of area in the northwest of China; that is, the expansion of the leading edge. This study is consistent with most of the results from similar research, such as on *Hippophae rhamnoides* subsp. *Sinensis* (Huang et al., 2018) and *Pinus tabuliformis* (Li et al., 2016). Besides, future climate change will lead to a loss in area of the southern boundary of Chinese ash; that is, its trailing edge shrinks. However, the shrink area of trailing edge is smaller than the expansion area of leading edge in total range. In total, the overall area of Chinese ash trees is large and will continue to increase in the future, which means that Chinese ash do not face the danger of extinction according to the theory of species–area curves (Thomas et al., 2004). When undertaking the adaptive management of Chinese ash to cope with climate change, the enhancement of dispersal ability of individual tree species, such as building corridors, artificial introductions, etc., should be performed more priority near the leading edge than that of the trailing edge.

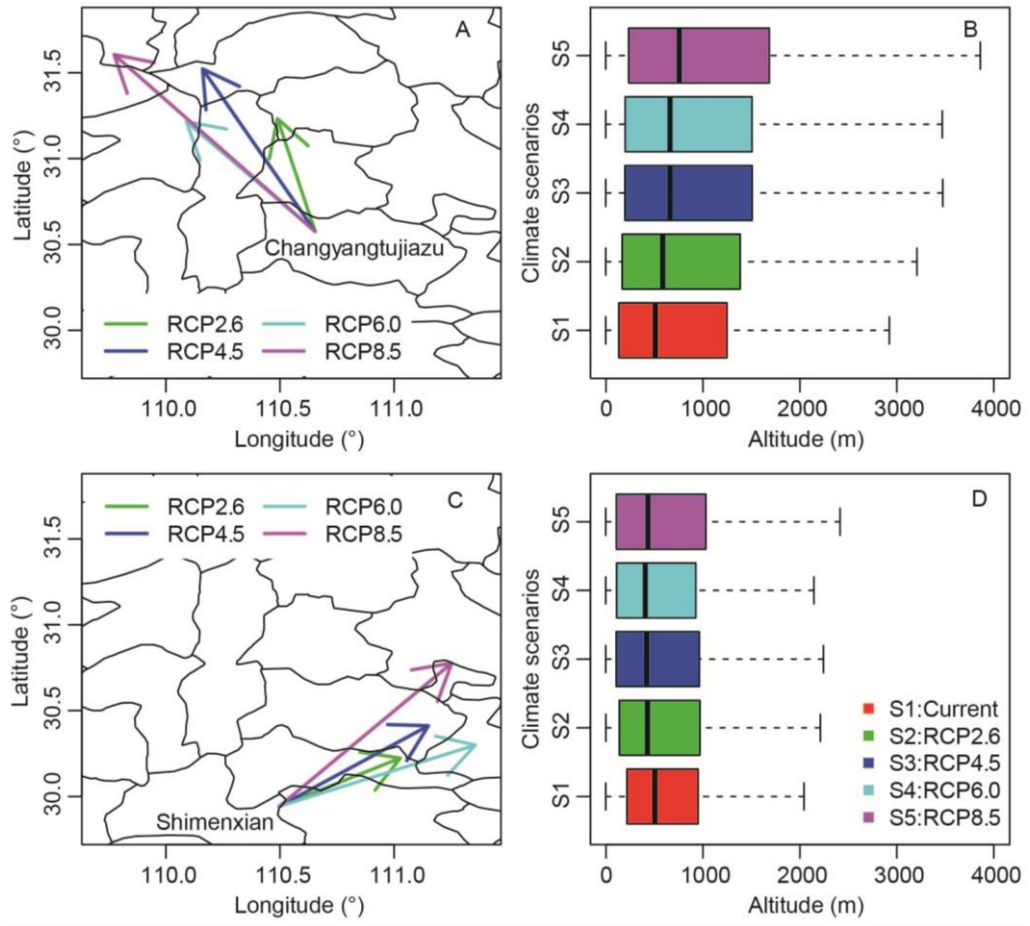

Figure 3. *Total range shift of ash in horizontal (A) and vertical (B) gradients; core range shift of ash in horizontal (C) and vertical (D) gradients*

In contrast to the total range, the range size change of the core range has similar expansion dynamics with it. However, the change in core range is more drastic than total range, especially for the proportion of expansion area. The loss area for the core

http://www.aloki.hu ● ISSN 1589 1623 (Print) ● ISSN 1785 0037 (Online)
DOI: http://dx.doi.org/10.15666/aeer/2005_44994513

range and the total range are small, and the average loss area is about 0.18×10^6 km^2 across climate scenarios. But, the expansion area in the core range is 37.5-75% more than that in total range, and the average expansion area for the core range is 0.9×10^6 km^2 across climate scenarios. It means that the core range is more sensitive to climate change than that for the total range. It also means that future climate change is conducive to the survival of this species from the perspective of climate suitability. The degree of benefits is increasing with the increase of CO2 concentration path. It means that future climate change will bring more opportunities to reforestation in high CO2 concentration path than that in low CO2 concentration path. Species range shift is the better way to adapt to climate change than plasticity and gene mutation (Aitken et al., 2008). But how fast and in which direction should Chinese ash adapts to climate change in three-dimensional geographical space in the late 21st century?

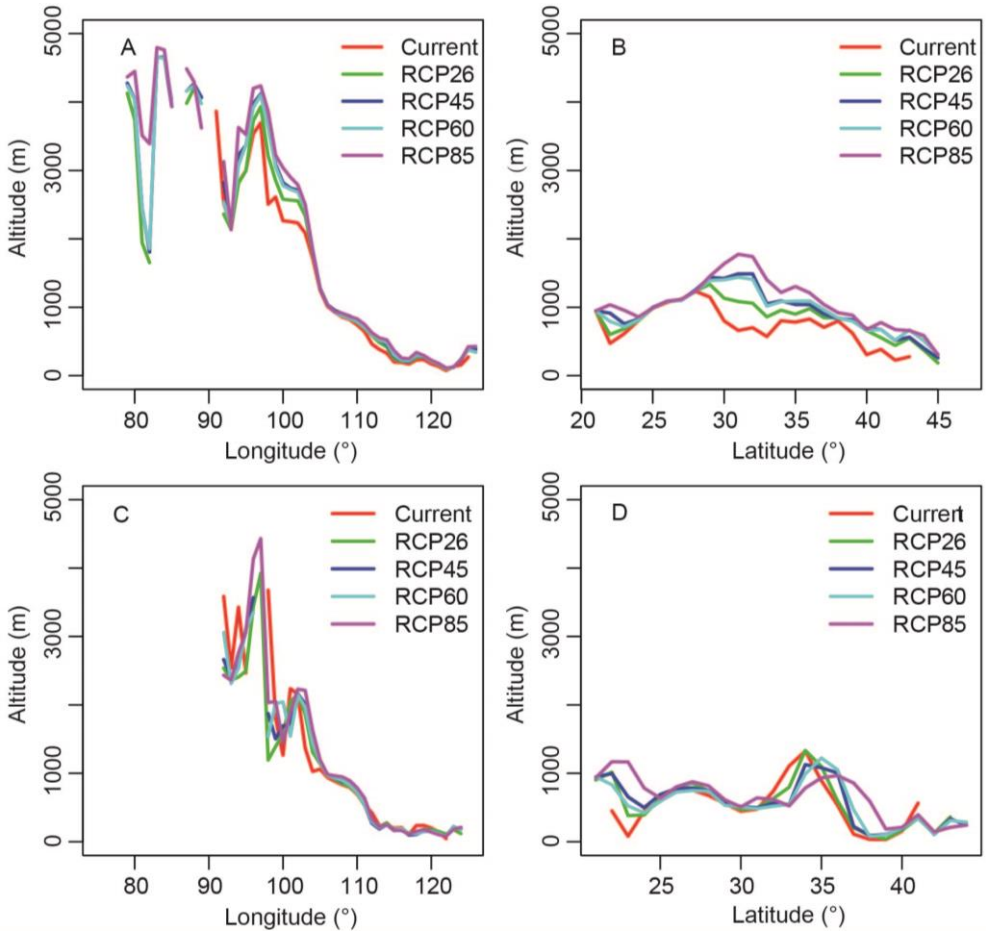

Figure 4. *Altitude centroid shifts in total range along the longitudinal (A) and latitudinal (B) gradients; altitude centroid shifts in core range along the longitudinal (C) and latitudinal (D) gradients*

Our study suggested that the shift velocity of range for Chinese ash is relatively slow at the horizontal gradients, reaching only 6.30–12.33 km/decade to northeast for core range and 7.86–14.92 km/decade to northwest for total range. One reason may be that Chinese ash occupies a wider climate niche and the driving factor of range shift is mainly the expansion of the leading edge rather than the contraction from the trailing edge. At the

http://www.aloki.hu ● ISSN 1589 1623 (Print) ● ISSN 1785 0037 (Online)
DOI: http://dx.doi.org/10.15666/aeer/2005_44994513

same time, we should note that although the shift velocity of the total range is similar to that of the core range, the direction of the range shift is not strictly following the shift to poleward or northward. This is inconsistent with the traditional understanding (Chen et al., 2011; Lenoir and Svenning, 2015). Traditionally, species should shift to the north to track the constancy of temperature (Burrows et al., 2014). This traditional understanding was based on the assumption that temperature is the main limit climatic factor affecting species distribution. However, this study found that annual precipitation is still one of the limiting factors for Chinese ash. Our research did not support this hypothesis, so the shift direction of the core range and the total range is different from the traditional northward viewpoint. It indicated that simply considering poleward or northward shift will underestimate the actual shift velocity of Chinese ash species (underestimating about 2.2-20.1% for total range and 21.2-56.3% for core range).

On the altitude gradient, we found that the altitude centroid of the total range will increase slightly with a velocity of 8.2–26.1 m/decade, but that of the core range will decrease slightly with a velocity of -10.5 – -7.6 m/decade in the future scenarios. This means that the shift direction of the core range and the total range on the vertical gradient is completely opposite. The shift direction of the core range challenges the traditional understanding (upward shift) to a certain extent (Lenoir et al., 2008). The shift direction of core range was simulated to downward, which may be related to the increase in annual precipitation in low-altitude areas along the eastern coast of China, and then the increase in annual precipitation offsets the potential threat of temperature rise to the suitability of Chinese ash (Harsch et al., 2016; Huang et al., 2018). Downward shifts also mean that Chinese ash may face more intense interference from persistent human activities in the future, especially land use change. Therefore, much attention should be focused on both the impact of climate change and land use on suitability of Chinese ash in the future studies.

Uncertainty and future efforts

The modern bioclimatic envelope model began with the development of the BIOCLIM program in 1984 (Booth et al., 2014). The development of improved methods of climatic interpolation as part of the BIOCLIM project has allowed reliable estimates to be made for locations that are some distance from existing meteorological stations across the whole world (Hijmans et al., 2005; Fick and Hijmans, 2017). Important advances are now being made with providing data on soil conditions across the world (Booth, 2018). However, extensive testing will be required before the reliability of these data is determined for China. Besides, soil factors cannot be obtained in the future, which also limits the use of soil factors as prediction variables. Here we have concentrated on determining the climate niche and dimensions of potential ranges for Chinese ash under current and future scenarios. These range maps may be overestimated the range of the species according to Eltonian Noise Hypothesis, which believes that limitation of small-resolution factors (e.g. soil factors) can be papered over on large-resolution (Soberon and Nakamura, 2009). Therefore, the range shift maps should assist managers' plan the rational conservation and use of Chinese ash under changing climates. Currently, a large amount of free land use and disturbance data can be obtained (Chen et al., 2017; Mu et al., 2022). Combined with our predicted range maps and these land use and disturbance data, a further detailed planning can be realized. Thus, it is conducive to climate suitability decision-making.

http://www.aloki.hu ● ISSN 1589 1623 (Print) ● ISSN 1785 0037 (Online)
DOI: http://dx.doi.org/10.15666/aeer/2005_44994513

Species velocity based on projections of changes in climatic niche alone (as is the case here) does not inform about species' dispersal ability. Aubin et al. (2016) defined tree dispersal ability as seed dispersal distance, dispersal vector and seed mass. Instead, species velocity as defined here was a way of quantifying species exposure to climate change (Glick et al., 2011). The inherent assumption of this research was that species has infinite dispersal capacity. However, in reality, it is difficult for species to achieve such a situation under natural conditions and further research is needed on whether the species can keep up with the pace of climate change. Interestingly, human assistant migration, such as afforestation and planting trees, could enhance the dispersal ability of species and this can break through the limit of tree migration. Numerous afforestation and greening projects have been carried out in China (Bran et al., 2018) and the species can play an important role in vegetation greening and construction. Our study provides significance guiding for the specific shift direction of planting tree species in response to future climate change, thus determining the potential shift route and adjust the shift speed.

Conclusion

We developed an indicator system to characterize the range shift of the total and core ranges of *Fraxinus chinensis* at three geographical dimensions under future climate change using the bioclimatic model and centroid methods. We found that the current core range and total range areas were 1.3×10^6 km^2 and 3.3×10^6 km^2, accounting for 13.5% and 34.4% of the country's land area. The core range and total range areas will increase under future climate change scenarios. The centroid shift velocity and direction of the core and the total ranges are 6.30–12.33 km/decade to northeast and 7.86–14.92 km/decade to northwest at the horizontal gradient. The driving force of range shift of the core and total ranges mainly comes from the expansion of the leading edge rather than the retreat of the trailing edge. At the vertical gradient, the shift direction of altitude in the total range is upward (8.2–26.1 m/decade), while the shift direction of altitude in the core range is downward (-10.5 – -7.6 m/decade). This study indicates that the response of total range and core distribution range to climate change is not synchronous. Simply considering poleward or northward shift will underestimate about 2.2–20.1% for total range and 21.2–56.3% for core range. Thus, the study has important guiding significance for determining the potential shift route and adjust the shift speed for planting the tree species in response to future climate change. The indicator system used has a wide range of practicability and can be applied to any species, region, or time.

Acknowledgements. The project was supported financially by National Natural Science Foundation of China (31971488).

REFERENCES

[1] Aitken, S. N., Yeaman, S., Holliday, J. A., Wang, T., Curtis-McLane, S. (2008): Adaptation, migration or extirpation: climate change outcomes for tree populations. – Evolutionary Applications 1: 95-111.

[2] Aubin, I., Munson, A. D., Cardou, F., Burton, P. J., Isabel, N., Pedlar, J. H., Paquette, A., Taylor, A. R., Delagrange, S., Kebli, H., Messier, C., Shipley, B., Valladares, F., Kattge, J., Boisvert-Marsh, L., McKenney, D. (2016): Traits to stay, traits to move: a review of

http://www.aloki.hu ● ISSN 1589 1623 (Print) ● ISSN 1785 0037 (Online)
DOI: http://dx.doi.org/10.15666/aeer/2005_44994513

functional traits to access sensitivity and adaptive capacity of temperate and boreal trees to climate change. – Environmental Reviews 24: 164-186.
[3] Booth, T. H. (2016): Estimating potential range and hence climatic adaptability in selected tree species. – Forest Ecology Management 366: 175-183.
[4] Booth, T. H. (2018): Why understanding the pioneering and continuing contributions of BIOCLIM to species distribution modelling is important. – Austral Ecology 43: 852-860.
[5] Booth, T. H., Nix, H. A., Busby, J. R., Hutchinson, M. F. (2014): BIOCLIM: the first species distribution modelling package, its early applications and relevance to most current MAXENT studies. – Diversity and Distribution 20: 1-9.
[6] Bryan, B. A., Gao, L., Ye, Y. Q., Sun, X. F., Connor, J. D., Crossman, N. D., Stafford-smith, M., Wu, J., He, C., Yu, D., Liu, Z., Li, A., Huang, Q., Ren, H., Deng, X., Zheng, H., Niu, J., Han, G., Hou, X. (2018): China's response to a national land-system sustainability emergency. – Nature 559: 193-204.
[7] Burrows, M. T., Schoeman, D. S., Richardson, A. J., Molinos, J. G., Hoffmann, A., Buckley, L. B., Moore, P. J., Brown, C. J., Bruno, J. F., Duarte, C. M., Halpern, B. S., Hoegh-Guldberg, O., Kappel, C. V., Kiessling, W., O'Connor, M. I., Pandolfi, J. M., Parmesan, C., Sydeman, W., Ferrier, S., Williams, K. J., Poloczanska, E. S. (2014): Geographical limits to species-range shifts are suggested by climate velocity. – Nature 507: 492-495.
[8] Chen, I. C., Hill, J. K., Ohlemuller, R., Roy, D. B., Thomas, C. D. (2011): Rapid range shifts of species associated with high levels of climate warming. – Science 333: 1024-1026.
[9] Chen, B.; Xu, B.; Zhu, Z.; Yuan, C.; Suen, H. P.; Guo, J.; Xu, N.; Li, W.; Zhao, Y.; Yang, J. (2019): Stable classification with limited sample: transferring a 30-m resolution sample set collected in 2015 to mapping 10-m resolution global land cover in 2017. – Science Bulletin 64: 370-373.
[10] DFRPSAASE (1994): Delectis Florae Reipublicae Popularis Sinicae Agendae Academiae Sinicae Edita. – In: Flora Reipublicae Popularis Sinicae. Science Press, Beijing.
[11] Diao, Z. E., Ding, F. B. (2004): Occurrence and control of white-stiped longhorn, *Batocera horsfildi* (Hope) (Coleoptera: Cerambycidae) on Chinese ash, *Fraxinus chinese* Roxb. – Entomological Journal of East China 13: 49-52.
[12] Elith, J., Phillips, S. J., Hastie, T., Dudik, M., Chee, Y. E., Yates, C. (2010): A statistical explanation of MaxEnt for ecologists. – Diversity and Distribution 17: 43-57.
[13] Fick, S. E., Hijmans, R. J. (2017): WorldClim 2: new 1 km spatial resolution climate surfaces for global land areas. – International Journal of Climatology 37: 4302-4315.
[14] Fielding, A. H., Bell, J. F. (1997): A review of methods for the assessment of prediction errors in conservation presence/absence models. – Environmental Conservation 24: 38-49.
[15] Geest, K., Sherbinin, A., Kienberger, S., Zommers, Z., Sitati, A., Roberts, E., James, R. (2019): The Impacts of Climate Change on Ecosystem Services and Resulting Losses and Damages to People and Society. In: Mechler, R., Bouwer, L., Schinko, T., Surminski, S., Linnerooth-Bayer, J. (eds.) Loss and Damage from Climate Change. Climate Risk Management, Policy and Governance. – Springer, Cham.
[16] Glick, P., Stein, B. A., Edelson, N. A. (2011): Scanning the Conservation Horizon: A Guide to Climate Change Vulnerability Assessment. – National Wildlife Federation, Washington, DC.
[17] Gobeyn, S., Mouton, A. M., Cord, A. F., Kaim, A., Volk, M., Goethals, P. (2019): Evolutionary algorithms for species distribution modelling: a review in the context of machine learning. – Ecological Modelling 392: 179-195.
[18] Harsch, M. A., HilleRisLambers, J. (2016): Climate warming and seasonal precipitation change interact to limit species distribution shifts across western North America. – PLoS ONE 11: e0159184.

http://www.aloki.hu ● ISSN 1589 1623 (Print) ● ISSN 1785 0037 (Online)
DOI: http://dx.doi.org/10.15666/aeer/2005_44994513

[19] Hijmans, R. J., Cameron, S. E., Parra, J. L., Jones, P. G., Jarvis, A. (2005): Very high resolution interpolated climate surfaces for global land areas. – International Journal of Climatology 25: 1965-1978.
[20] Holdridge, L. R. (1947): Determination of world plant formations from simple climatic data. – Science 105: 367-368.
[21] Huang, Q. Y., Sauer, J. R., Dubayah, R. O. (2017): Multidirectional abundance shifts among North American birds and the relative influence of multifaceted climate factors. – Global Change Biology 23: 3610-3622.
[22] Huang, J. H., Li, G. Q., Li, J., Zhang, X. Q., Yan, M. J., Du, S. (2018): Projecting the range shifts in climatically suitable habitat for Chinese sea buckthorn under climate change scenarios. – Forests 9: 9.
[23] Iverson, L. R., Prasad, A. M., Matthews, S. N., Peters, M. (2008): Estimating potential habitat for 134 eastern US tree species under six climate scenarios. – Forest Ecology and Management 254: 390-406.
[24] Kira, T. (1945): A New Classification of Climate in Eastern Asia as the Basis for Agricultural Geography. – Horticultural Institute, Kyoto University, Japan.
[25] Kosanic, A., Kavcic, I., vanKleunen, M., Harrison, S. (2019): Climate change and climate change velocity analysis across Germany. – Scientific Reports 9: 2196.
[26] Lafleur, B., Pare, D., Munson, A. D., Bergeron, Y. (2010): Response of northeastern North American forests to climate change: will soil conditions constrain tree species migration. – Environmental Reviews 18: 279-289.
[27] Lenoir, J., Gegout, J. C., Marquet, P. A., de Ruffray, P., Brisse, H. (2008): A significant upward shift in plant species optimum elevation during the 20th century. – Science 320: 1768-1771.
[28] Lenoir, J., Svenning, J. C. (2015): Climate-related range shifts - a global multidimensional synthesis and new research directions. – Ecography 38: 15-28.
[29] Li, G. Q., Xu, G. H., Guo, K., Du, S. (2016): Geographical boundary and climatic analysis of *Pinus tabulaeformis* in China: insights on its afforestation. – Ecological Engineering 86: 75-84.
[30] Li, G. Q., Zhang, X. Q., Huang, J. H., Wen, Z. M., Du, S. (2018): Afforestation and climatic niche dynamics of black locust (*Robinia pseudoacacia*). – Forest Ecology Management 407: 184-190.
[31] Li, G., Huang, J., Guo, K., Du, S. (2020): Projecting species loss and turnover under climate change for 111 Chinese tree species. – Forest Ecology and Management 477: 118488.
[32] Li, G., Paul, C. R., Huang, J. (2021): Black locust (*Robinia pseudoacacia* L.) range shifts in China: application of a global model in climate change futures. – Climate Change Ecology 2: 100036.
[33] Ma, J. (2022): Occurrence and control measures of diseases and pests for *Fraxinus chinensis*. – Seed Science and Technology 8: 82-84.
[34] Mu, H., Li, X., Wen, Y., Huang, J., Du, P., Su, W., Miao, S., Geng, M. (2018): A global record of annual terrestrial Human Footprint dataset from 2000 to 2018. – Scientific Data 9: 176.
[35] Peterson, A. T., Soberon, J., Pearson, R. G., Andersen, R. P., Martinez-Meyer, E., Nakamura, M., Araujo, M. B. (2011): Ecological Niches and Geographic Distributions; Monographs in Population Biology. No. 49. – Princeton University Press, Princeton, NJ.
[36] Phillips, S. J., Anderson, R. P., Schapire, R. E. (2006): Maximum entropy modeling of species geographic distributions. – Ecology Modelling 190: 231-259.
[37] Ren, H. (2022): Key points of *Fraxinus chinensis* afforestation technology. – World Tropical Agricultural Information 4: 41-42.
[38] Robinson, L. M., Hobday, A. J., Possingham, H. P., Richardson, A. J. (2015): Trailing edges projected to move faster than leading edges for large pelagic fish habitats under climate change. – Deep-Sea Res Pt Ii 113: 225-234.

http://www.aloki.hu ● ISSN 1589 1623 (Print) ● ISSN 1785 0037 (Online)
DOI: http://dx.doi.org/10.15666/aeer/2005_44994513

[39] Soberon, J., Nakamura, M. (2009): Niches and distributional area: concepts, methods, and assumptions. – Proceedings of the National Academy of Sciences of the United States of America 106: 19644-19650.
[40] Thomas, C. D., Cameron, A., Green, R. E., Bakkenes, M., Beaumont, L. J., Collingham, Y. C., Erasmus, B. F. N., de Siqueira, M. F., Grainger, A., Hannah, L., Hughes, L., Huntley, B., van Jaarsveld, A. S., Midgley, G. F., Miles, L., Ortega-Huerta, M. A., Peterson, A. T., Phillips, O. L., Williams, S. E. (2004): Extinction risk from climate change. – Nature 427: 145-148.
[41] Wang, H. J., Dai, J. H., Ge, Q. S. (2012): The spatiotemporal characteristics of spring phenophase changes of *Fraxinus chinensis* in China from 1952-2007. – Science China Earth Science 55: 991-1000.
[42] Xu, S. Y., Ye, J. F. (2014): Advances in research on tree reproduction of Chinese ash (*Fraxinus chinensis*). – Protection Forest Science and Technology 2: 44-45.
[43] Yang, X. J., Wang, X. K. (2019): Regional difference of urbanization speed in China and its main influencing factors. – Ecological Science 38: 36-44.
[44] Zhang, L. J., Shen, H. L., Cui, J. G., Zhou, Q. (2007): Advances in somatic embryogenesis of *Fraxinus* species. – Biotechnology Bulletin 3: 31-34.
[45] Zhang, W., Brandt, M., Penuelas, J., Guichard, F., Tong, X., Tian, F., Fensholt, R. (2019): Ecosystem structural changes controlled by altered rainfall climatology in tropical savannas. – Nature Communications 10: 671.
[46] Zhang, Z. G., Li, B., Shi, K. Q., Yang, J. J., Wang, H. P., Li, H., Shi, H. Y. (2022): Response of five introduced *Fraxinus chinensis* species to drought stress in Yili area. – Agricultural Research in the Arid Areas 2: 9-16.

http://www.aloki.hu ● ISSN 1589 1623 (Print) ● ISSN 1785 0037 (Online)
DOI: http://dx.doi.org/10.15666/aeer/2005_44994513